Electronic Supplementary Material (ESI) for Dalton Transactions.

Supporting Information

First principles prediction of two-dimensional Janus $STiXY_2$ (X = Si, Ge; Y=N, P, As) materials

Zhen Gao[a] , Xin He[a] , Wenzhong Li[a] , YaoHe[a,*], and Kai Xiong[b]

[a]*Department of Physics, Yunnan University, Kunming 650091, People's Republic of China.*

[b]*Materials Genome Institute, School of Materials and Energy, Yunnan University, Kunming 650091, P. R. China.*

*E-mail:
yhe@ynu.edu.cn

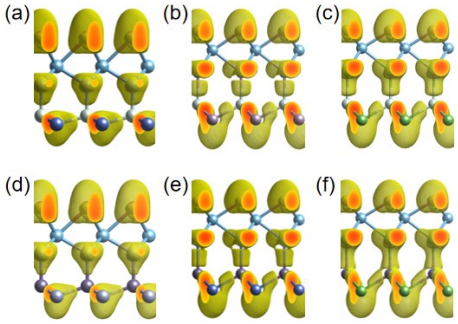

Fig S1 The electron localization function (ELF) for 2D Janus (a) $STiSiN_2$, (b) $STiSiP_2$, (c) $STiSiAs_2$, (d) $STiGeN_2$, (e) $STiGeP_2$, and (f) $STiGeAs_2$ monolayers.. The isosurface for ELF is 0.75 $eÅ^{-3}$.

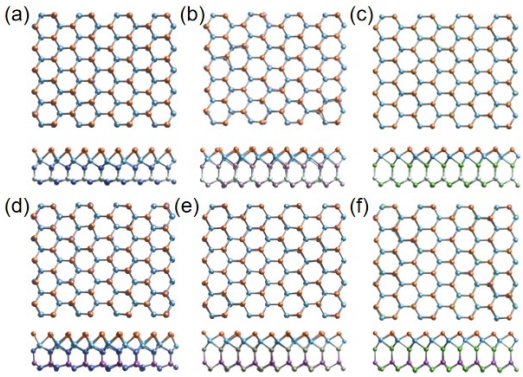

Fig S2 Ab initio molecular dynamics (AIMD) simulation results at 300 K for 2D Janus (a) $STiSiN_2$, (b) $STiSiP_2$, (c) $STiSiAs_2$, (d) $STiGeN_2$, (e) $STiGeP_2$, and (f) $STiGeAs_2$ monolayers.

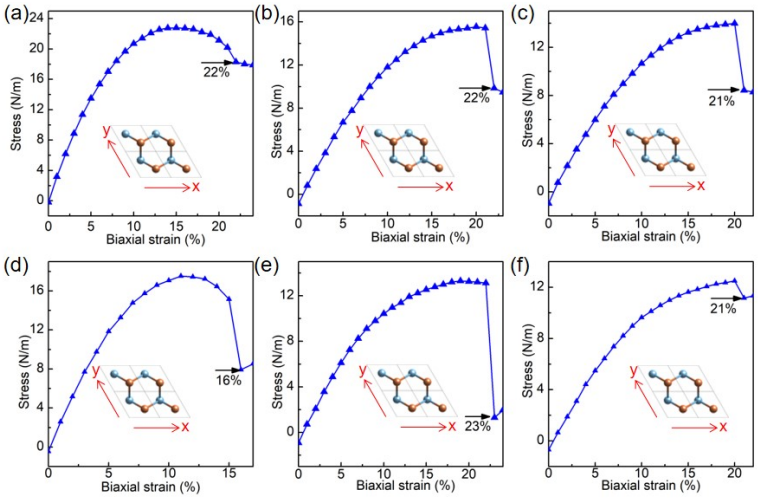

Fig S3 strain-stress curve for for 2D Janus (a) $STiSiN_2$, (b) $STiSiP_2$, (c) $STiSiAs_2$, (d) $STiGeN_2$, (e) $STiGeP_2$, and (f) $STiGeAs_2$ monolayers.

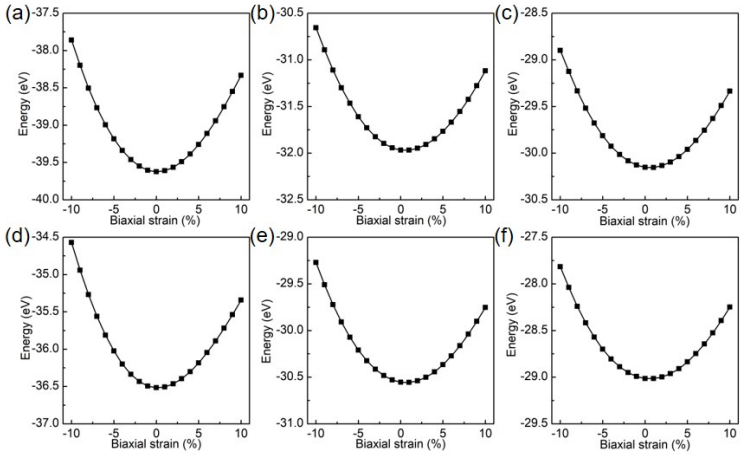

Fig S4 Energy-strain curves of for 2D Janus (a) $STiSiN_2$, (b) $STiSiP_2$, (c) $STiSiAs_2$, (d) $STiGeN_2$, (e) $STiGeP_2$, and (f) $STiGeAs_2$ monolayers.

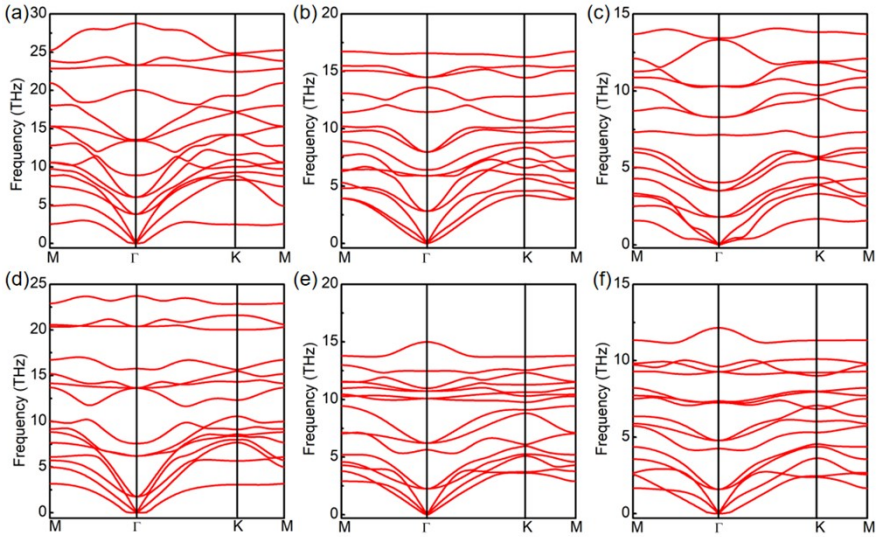

Fig S5 Phonon spectrum of (a) $STiSiN_2$, (b) $STiSiP_2$, (c) $STiSiAs_2$, (d) $STiGeN_2$, (e) $STiGeP_2$, and (f) $STiGeAs_2$ monolayers under strain of -10 % .

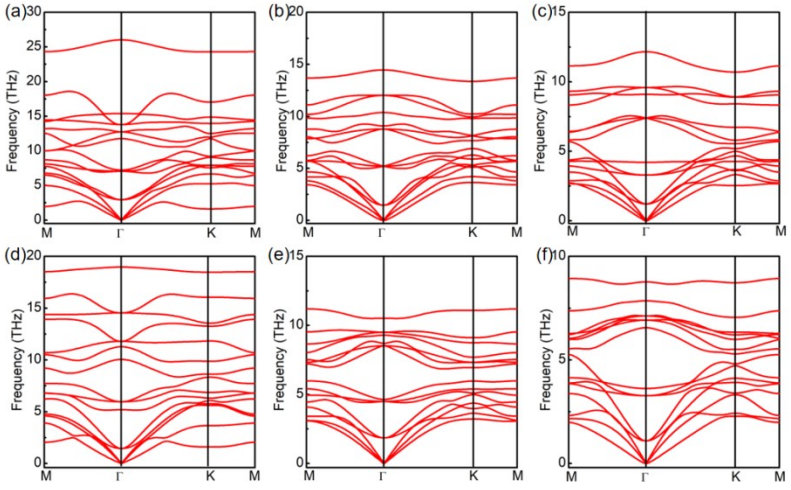

Fig S6 Phonon spectrum of (a) $STiSiN_2$, (b) $STiSiP_2$, (c) $STiSiAs_2$, (d) $STiGeN_2$, (e) $STiGeP_2$, and (f) $STiGeAs_2$ monolayers under strain of +10 % .

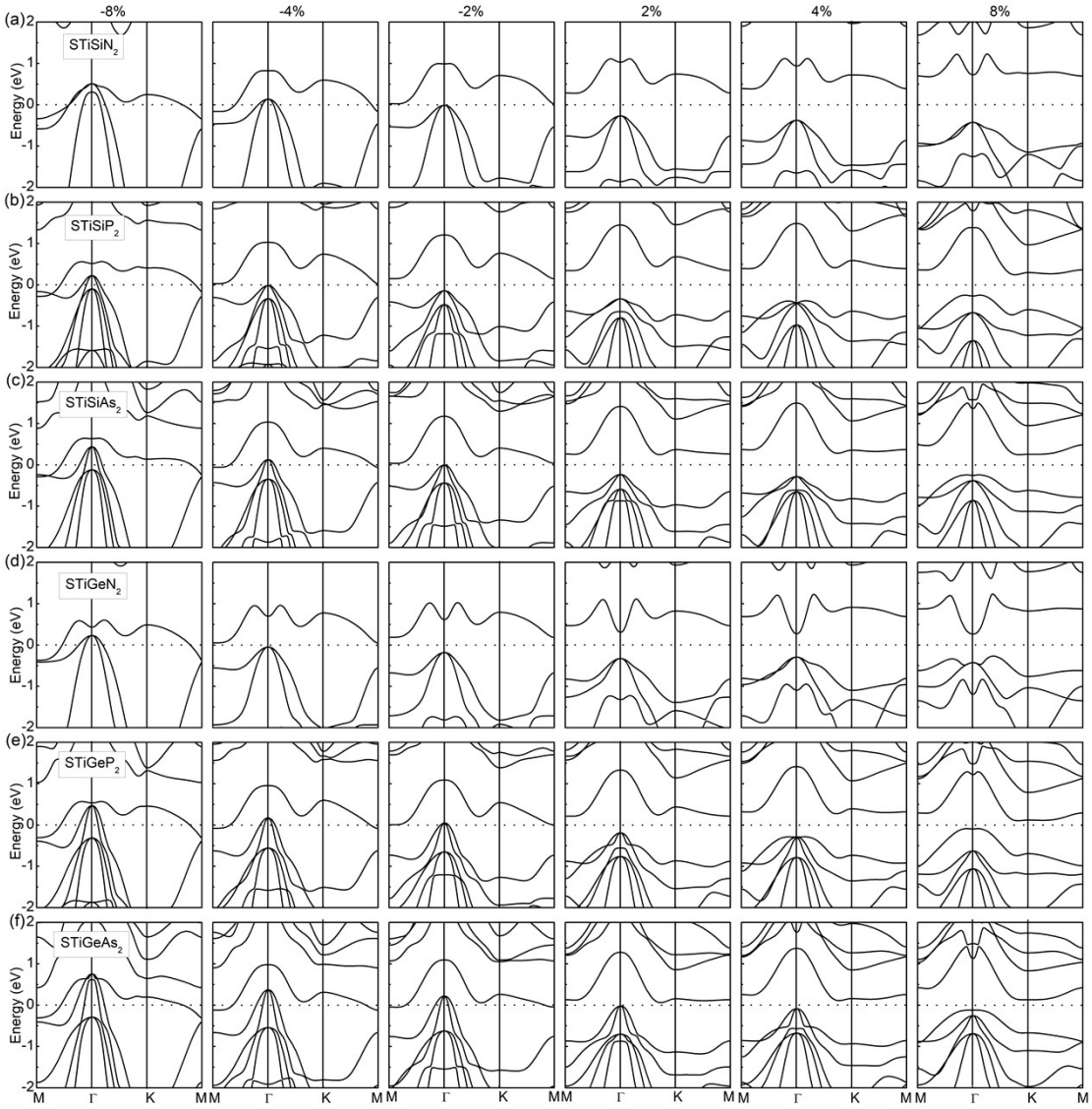

Fig S7 Electronic band structure under biaxial strain of 2D Janus (a) $STiSiN_2$, (b) $STiSiP_2$, (c) $STiSiAs_2$, (d) $STiGeN_2$, (e) $STiGeP_2$, and (f) $STiGeAs_2$ monolayers.

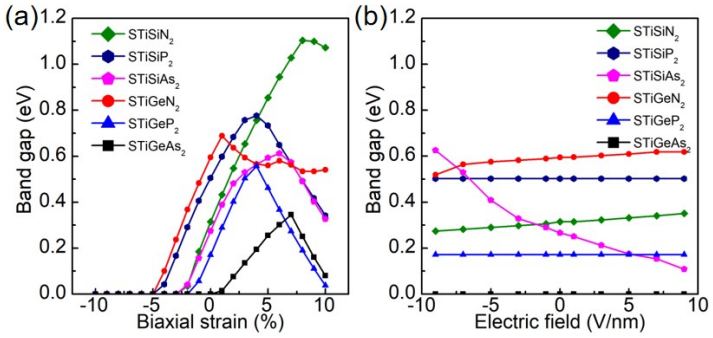

Fig S8 Band gaps under (a) strain and (b) external electric field of 2D Janus $STiSiXY_2$(X =Si, Ge; Y= N, P, As) by PBE method.

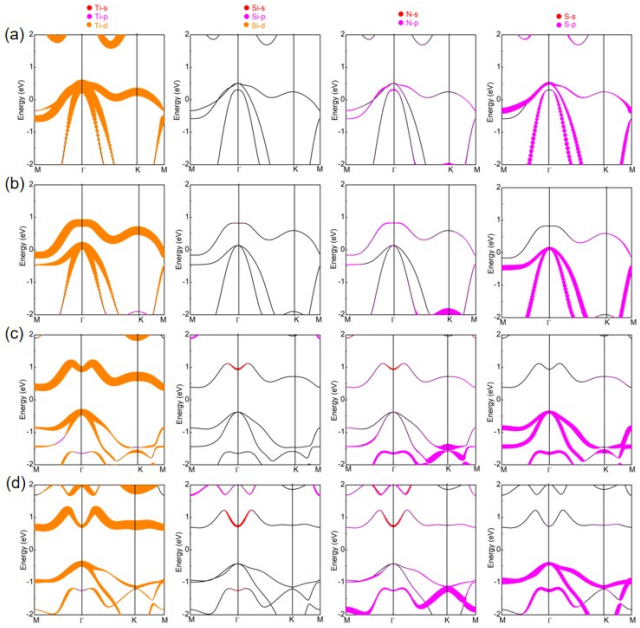

Fig S9 Orbital projected band structures for $STiSiN_2$ monolayer under different strengths of different strains of (a) -8%, (b) -4%, (c) 4% and (d) 8%.

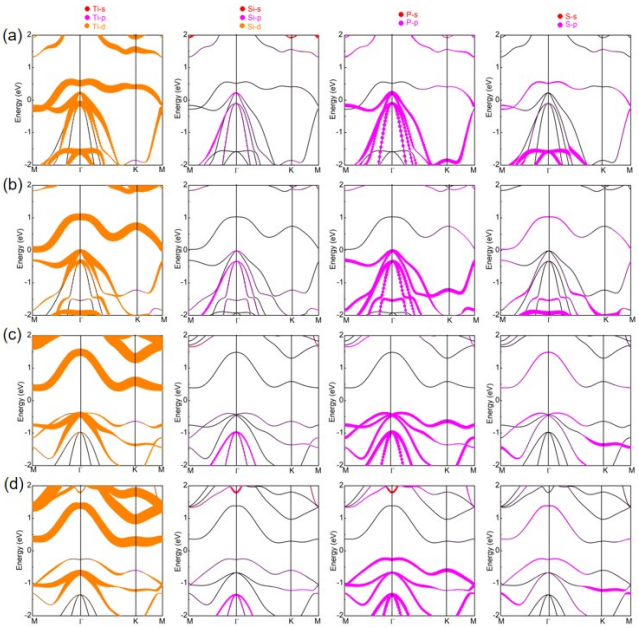

Fig S10 Orbital projected band structures for $STiSiP_2$ monolayer under different strengths of different strains of (a) -8%, (b) -4%, (c) 4% and (d) 8%.

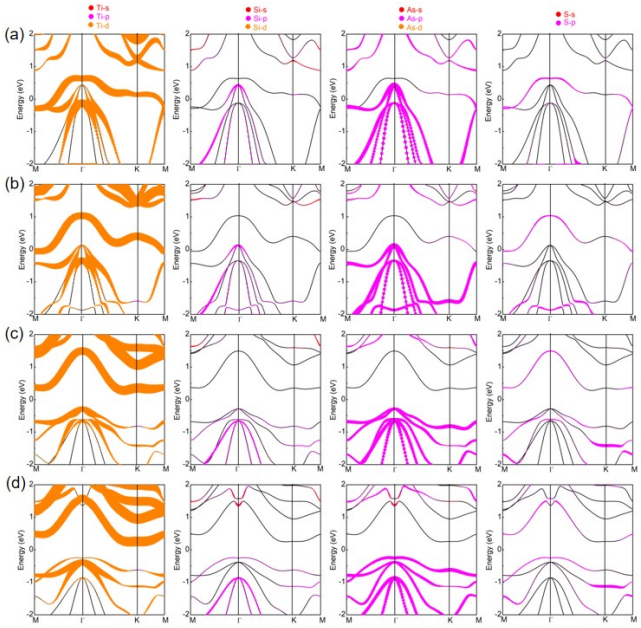

Fig S11 Orbital projected band structures for $STiSiAs_2$ monolayer under different strengths of different strains of (a) -8%, (b) -4%, (c) 4% and (d) 8%.

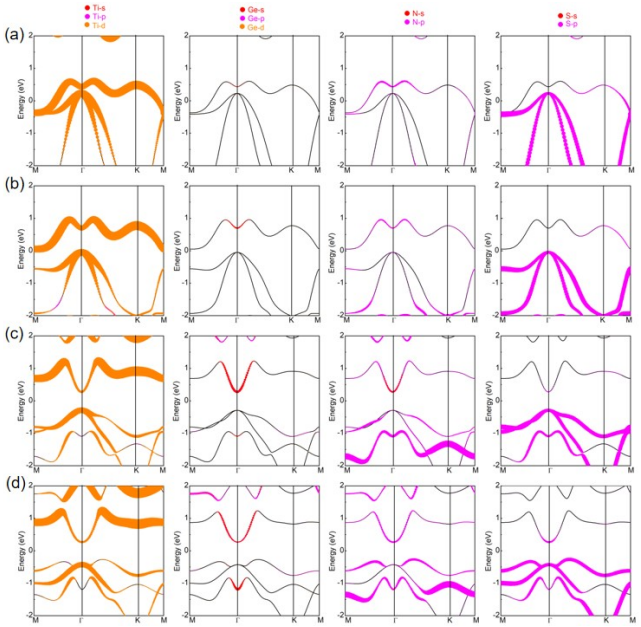

Fig S12 Orbital projected band structures for $STiGeN_2$ monolayer under different strengths of different strains of (a) -8%, (b) -4%, (c) 4% and (d) 8%.

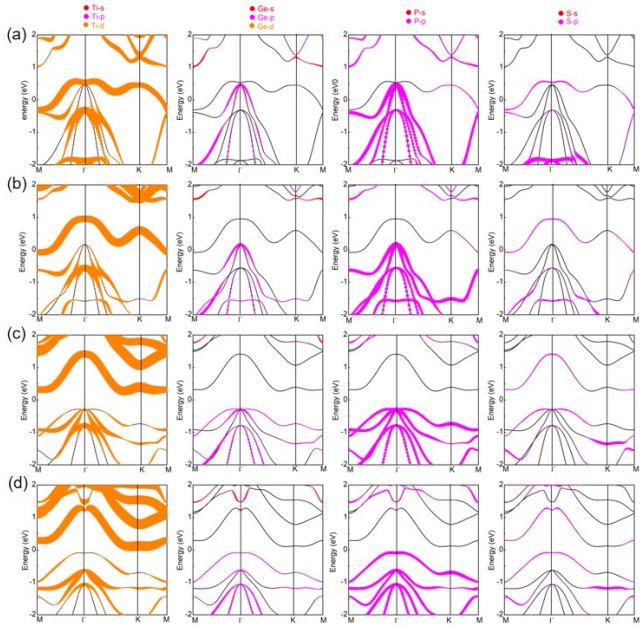

Fig S13 Orbital projected band structures for $STiGeP_2$ monolayer under different strengths of different strains of (a) -8%, (b) -4%, (c) 4% and (d) 8%.

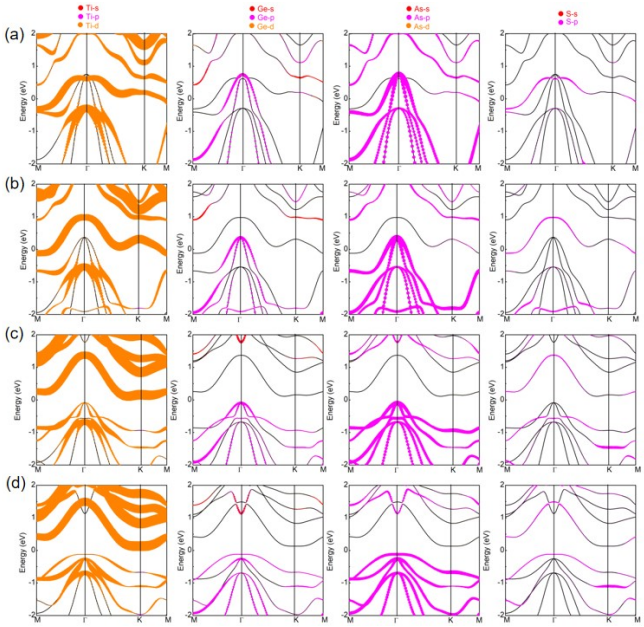

Fig S14 Orbital projected band structures for $STiGeAs_2$ monolayer under different strengths of different strains of (a) -8%, (b) -4%, (c) 4% and (d) 8%.

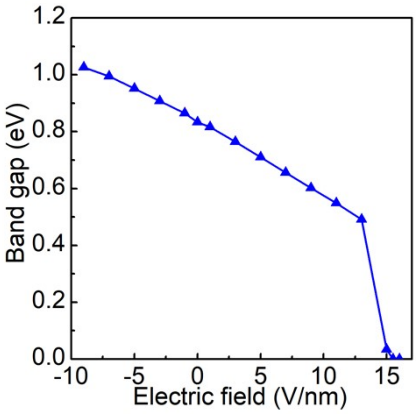

Fig S15 Band gaps under external electric field of 2D $STiSiAs_2$ by HSE method.

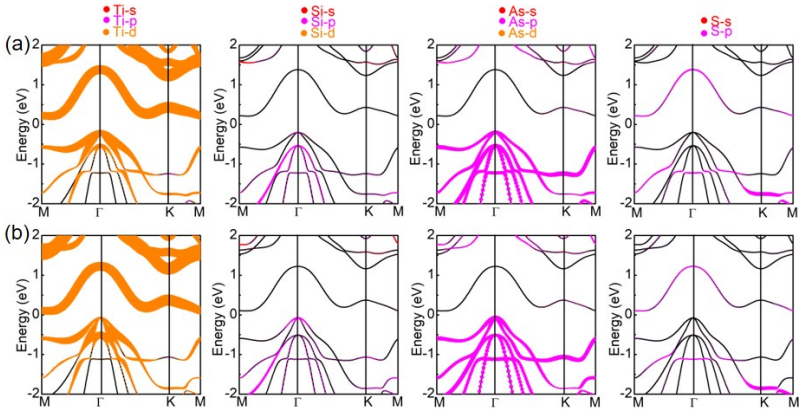

Fig S16 Orbital projected band structures for $STiSiAs_2$ monolayer under different strengths of electric field of (a) E = -5 V/nm and (b) E = 5 V/nm

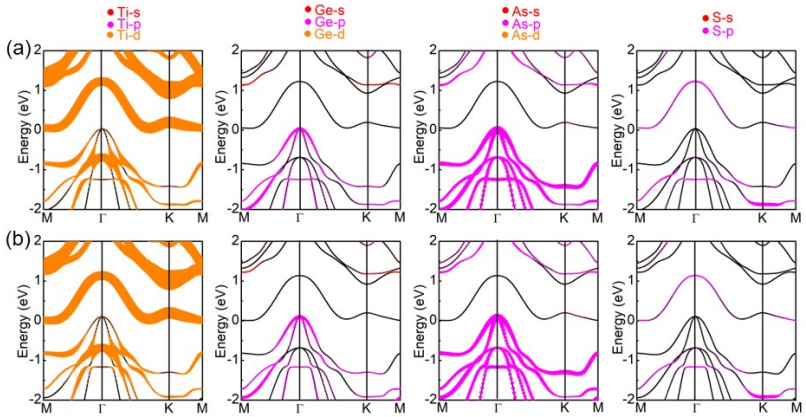

Fig S17 Orbital projected band structures for $STiGeAs_2$ monolayer under different strengths of electric field of (a) E = -5 V/nm and (b) E = 5 V/nm

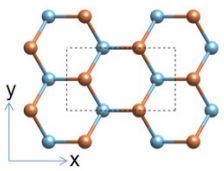

Fig S18 The calculation of carrier mobility is carried out in rectangular cell in the black dotted box, the x and y directions also been indicate.